International Journal of ChemTech Research
CODEN (USA): IJCRGG ISSN: 0974-4290
Vol.7, No.01, pp 269-274, 2014-2015

Spectroscopic Studies on Pure and Mn^{2+} Doped Nonlinear L-Cysteine Hydrochloride Monohydrate for Electro-optic Modulation

P.V. Prasad[1], T.K.V. Rao[1], S. Rajya Lakshmi[1], B. Brahmaji[1], K. Ramachandra Rao[1] and M.C. Rao[2]*

[1]Crystal growth and Nanoscience Research Centre, Department of Physics, Government College (A), Rajahmundry, A.P., India
[2]Department of Physics, Andhra Loyola College, Vijayawada-520 008, A.P., India

Abstract: Good quality single crystals of pure and organometallic complex nonlinear optical material Mn^{2+} doped L-Cysteine hydrochloride monohydrate (Mn^{2+}: L-Cys.HCl.H_2O) were grown by slow evaporation solution technique (SEST) at constant temperature. Powder X-ray diffraction (PXRD) pattern and FTIR spectra have been recorded to study variation in the lattice parameters and functional groups. High resolution X-ray diffraction (HRXRD) study revealed the effect of dopant on crystalline perfection. The influence of doping on optical transparency and SHG was investigated for the crystals. The second harmonic generation conversion efficiency of Mn^{2+}: L-Cys.HCl.H_2O have found 1.5 times of standard KDP. The S-H and C-S functional groups are directly involved in Mn^{2+} coordination through S-ligand in L-Cys.HCl H_2O and have promoted nonlinear optical efficiency.
Keywords: Mn^{2+}: L-Cys.HCl.H_2O, solution technique, PXRD, FTIR and optical efficiency.

Introduction:

Materials that possess the non-centrosymmetric are studied extensively for their possible applications. Especially, NLO crystal materials exhibit excellent applications such as laser frequency conversion, electro-optic switching and holographic data storage optical computing, optical information processing, color displays and medical diagnostics [1-3]. Amino acids are the molecular building blocks of peptides and proteins. The growth of amino acid crystals from aqueous solutions containing transition metal lays a solid foundation for understanding the role of transition metals in proteins. L-Cys.HCl.H_2O is promising NLO material from amino acid family to investigate because it crystallizes in orthorhombic structure with molecular formula $C_3H_7NO_2S$.HCl.H_2O with space group $P2_12_12_1$ [4]. The reported space group of L-Cys.HCl.H_2O indicates that the crystal is non-centrosymmetric and may possess NLO properties. L-Cysteine is sulphur-containing amino acid which is characterized by the presence of a mercaptogroup (-SH). The mercapto group has a high affinity for heavy metals, hence L-Cys.HCl.H_2O bind metals such as mercury, lead and cadmium tightly. The transition metal ions doped in L-Cys.HCl.H_2O crystals provide valuable information on the binding mechanism of metal in L-Cys. rich environments and the formation of phytochelatin metallothionein complexes [5]. In the cysteine molecule, the function groups, such as $–NH_2$, –COOH and –SH, have a strong tendency to coordinate with inorganic cations and metals, which has been demonstrated by Burford and co-workers on the basis of the observations of mass spectrometry [6]. As reported in many previous publications that incorporation of dopants in crystals leads to modification of the electric dipole-photon effect in the energy-matter interaction and make the crystal efficient for SHG [7-9]. Several research groups were published on different aspects of NLO crystals and demonstrated that metal ions enhance nonlinear effects by modifications in the crystalline lattice of photonic crystals [10]. The incorporation of Mn^{2+} ions modifies the NLO properties of crystals and greatly improves their data storage capability [11, 12]. Herein, we have intensive interest in the growth and

characterization of Mn^{2+} doped L-Cys.HCl.H_2O single crystal. The aim of the present communication is to study the influence of Mn^{2+} on the lattice parameters, crystalline perfection, functional groups, optical transparency, and SHG of Mn^{2+}: L-Cys.HCl.H_2O.

Experimental:

Crystal Growth:

Pure and Mn^{2+}: L-Cys.HCl.H_2O single crystals have been successfully grown by SEST at constant temperature. In both cases, double distilled water is used as a solvent. The saturated solution of pure L-Cys HCl.H_2O was prepared 30 ^oC with continuous stirring for 24 h. The solution was filtered and kept in a constant temperature bath (CTB) at 30 ^oC. Spontaneous nucleation resulted in growth of a few small sized good quality crystals. These were used subsequently for growth by slow evaporation technique in the temperature range of 30 – 35 °C with an increasing rate of 0.5°C/day. A bulk crystal of pure L-Cys HCl.H_2O with dimensions 15 × 12 × 5 mm^3 was harvested in 12 days. The grown crystal is shown in Fig. 1(a). To get Mn^{2+}: L-Cys HCl.H_2O single crystals, 1mol% amount of $MnCl_2$ was added to the saturated solution of L-Cy HCl.H_2O and again stirred for 24 h at 30 °C. The reaction takes place in the processes as follows:

$C_3H_7NO_2S.HCl.H_2O + MnCl_2 \rightarrow Mn\ (C_3H_7NO_2S.HCl.H_2O)\ Cl_2$

and the same procedure was followed as that of pure L-Cys. HCl.H_2O. The good transparent Mn^{2+}doped L-Cysteine HCl.H_2O with dimensions 21 × 20 × 7 mm^3 was obtained after a period of 14 days and the crystal is shown in Fig. 1(b).

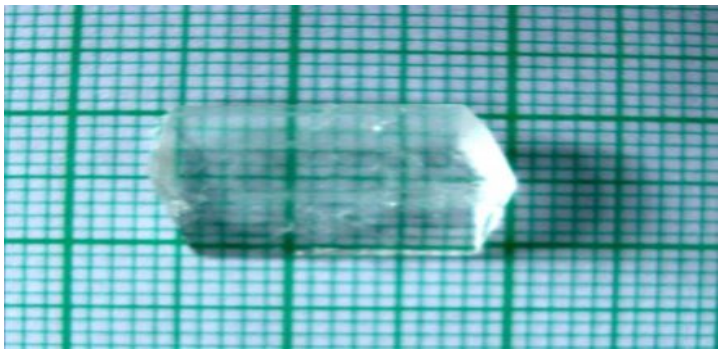

Fig. 1(a) Photograph of pure L-Cys. HCl.H_2O grown single Crystal

Fig. 1(b) Photograph of Mn^{2+}doped L-Cys. HCl.H_2O grown single Crystal

Characterization:

Powder XRD measurements were carried out using a PW1830 Philips Analytical X-ray diffractometer with nickel-filtered Cu K_α radiation (35 kV, 30 mA) at a scan rate 0.02 s^{-1} for the 2θ angular range of 10–60^o at room temperature. FTIR spectrum was also recorded in the range 400-4000cm^{-1} by using KBr pellet on Perkin Elmer RXI FTIR. To measure the SHG efficiency of Mn^{2+}: L-Cys HCl.H_2O single crystals, well crushed powders of the pure and doped crystals were filtered with a 25 mm standard test sieve to achieve homogeneous

particle size. These powders were densely packed into a glass micro-capillary of 1 mm bore and subjected to the Kurtz powder technique. A KDP crystal was used as a reference. An Nd: YAG laser of fundamental wavelength 1064 nm, pulse width 8 ns, with a repetition rate of 10 Hz was used in 90° scattering geometry as a source. The laser radiation was made incident on the specimen sample and green output radiation from the specimen was detected by a photomultiplier tube (PMT) coupled with a filter. The SHG signals of the specimen crystal and the standard KDP were recorded.

To evaluate the crystalline perfection of the specimen crystals, HRXRD analysis was carried out. A multicrystal X-ray diffractometer [13] was used to record high resolution rocking or diffraction curves (DCs). In this system, a fine focus (0.4 × 8 mm^2; 2 kW Mo) X-ray source energized by a well stabilized Philips X-ray generator (PW 1743) was employed. The well collimated and monochromatic MoKα_1 beam obtained from the three monochromator Si crystals set in dispersive (+, -, -) configuration has been used as the exploring X-ray beam. This arrangement improves the spectral purity ($\Delta\lambda/\lambda << 10^{-5}$) of the MoK$\alpha_1$ beam. The divergence of the exploring beam in the horizontal plane was estimated to be << 3 arc sec. The specimen crystal is aligned in the (+, -, -, +) configuration. Due to dispersive configuration of the third monochromator crystal with respect to the second monochromatic, the spectral quality of the diffracted beam emerged from the third monochromator is highly perfect ($\Delta\lambda/\lambda \sim 10^{-5}$; horizontal divergence >> 3 arc seconds) and hence though the lattice constant of the monochromator crystal and the specimen are different, the unwanted experimental dispersion broadening in the diffraction curve of the specimen crystal [$\Delta FWHM = \Delta\lambda/\lambda(\tan\theta_M - \tan\theta_S)$; θ_M and θ_S are being the Bragg diffraction angles of monochromator and the specimen crystals] is insignificant. The advantage of dispersion configuration (+, −, −) over the non-dispersive configuration (+, −, +) of monochromators is well described [14]. The specimen can be rotated about a vertical axis, which is perpendicular to the plane of diffraction, with minimum angular interval of 0.4 arc sec. The diffracted intensity is measured by using a scintillation counter. The DCs were recorded by changing the glancing angle around the Bragg diffraction peak position θ_B starting from a suitable arbitrary glancing angle (θ). The detector was kept at the same angular position $2\theta_B$ with wide opening for its slit, the so called ω scan. Before recording the diffraction curve, to remove the non-crystallized solute atoms remained on the surface of the crystal and also to ensure the surface planarity, the specimens were first lapped and chemically etched in a non-preferential etchant of water and acetone mixture in 1:2 volume ratios. The UV–vis spectra have been recorded using a spectrophotometer (Perkin Elmer Lambda-25) in the entire ultra- violet–visible region (200–900 nm) of wavelength, to check the transparency of pure and Mn: L-Cys.HCl.H_2O crystals.

Results and Discussion:

Powder X-ray Diffraction Analysis:

The Mn^{2+} doped L-Cys HCl H_2O single crystal is analyzed for its structure by recording the powder X-ray diffraction. The grown crystal belongs to orthorhombic system and space group is $P2_12_12_1$. The unit cell dimensions are a = 19.520 A^0, b = 7.039 A^0 and c= 5.714 A^0 which were calculated using POWDER X-refinement software and observed values shown in Table-1 are within the standard deviations [14].

Table-1 Lattice parameters of doped and undoped L-Cys.HCl.H_2O

Sample	a(A^0)	b(A^0)	c(A^0)	V(A^3)	Space Group
L-Cys (Pure)	19.480	7.120	5.520	765.611	$P2_12_12_1$
L-Cys (doped)	19.720	7.039	5.714	793.155	$P2_12_12_1$

The high-resolution diffraction curve (DC) recorded for pure and doped L-Cys.HCl.H_2O crystal using (110) diffracting planes in symmetrical Bragg geometry by employing the multicrystal X-ray diffractometer with MoK$\alpha_1$radiation shown in Fig.2. As shown in the figure, both the DCs contain a single peak and indicate that the specimens are free from structural grain boundaries. The FWHM (full width at half maximum) of the curves are 20 and 63 arc seconds which is somewhat more than that expected from the plane wave theory of dynamical X-ray diffraction [15].

High Resolution X-ray Diffraction:

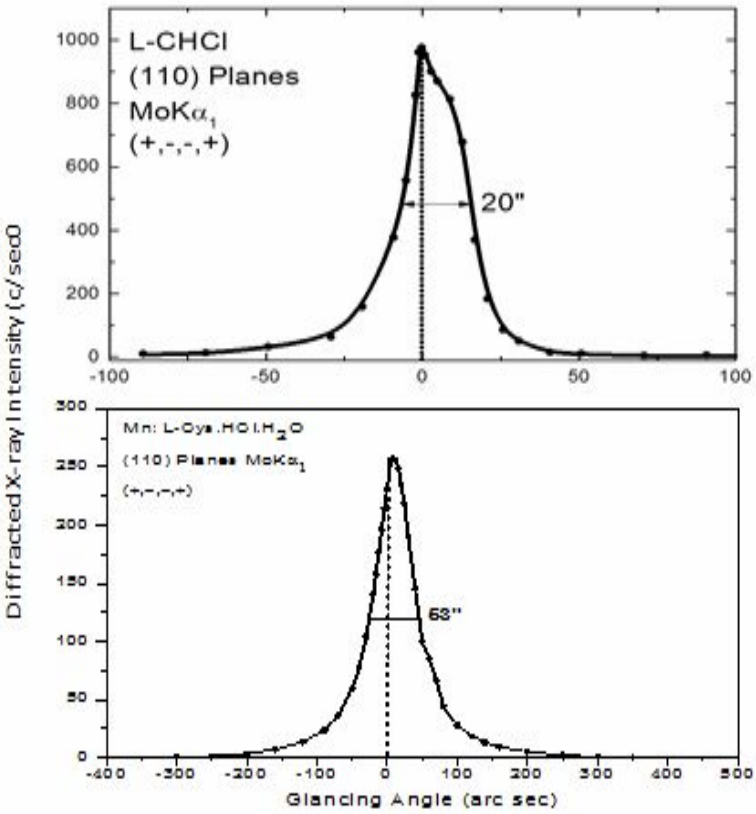

Fig. 2 Diffraction curves recorded for Mn^{2+}: L-Cys.HCl.H_2O and pure single crystal for (110) diffraction plane

In the case of pure L-Cysteine HCl.H_2O grown crystal, for a particular angular deviation ($\Delta\theta$) of glancing angle with respect to peak position, the scattered intensity is much greater in positive direction than in negative direction. This indicates predominantly interstitial type defect rather than vacancy defects. Due to the interstitial defects, the local sub-lattice around the defect core undergoes stress and the interplanar spacing d of the lattice around the defect core contracts. Such defects are very common to observe in almost all real crystals and are many times unavoidable due to thermodynamical conditions. More details may be obtained from the study of high resolution diffuse X-ray scattering measurements [16], which is not the main focus of the present investigation. Fig. 2 shows the recorded DC for Mn^{2+}: L-Cys.HCl.H_2O single crystal. The FWHM value is much higher than the undoped single crystal. This increase in the FHWM without having any multiple peaks due to doping indicates the distribution of Mn^{2+} doping in the lattice. It is interesting to find an asymmetry of the DC with respect to the peak position for a particular angular deviation ($\Delta\theta$), the scattered intensity in the positive direction is slightly larger than that in negative direction. This investigation clearly shows that the dopants occupy the interstitial sites in the crystal lattice. Due to incorporation of dopants in interstitial sites, the lattice around the dopants shows compressed stress and interplanar spacing'd' decreases [17].

FT-IR Analysis:

The recorded spectra of grown crystals are shown in Fig. 3. In the spectra peaks appeared at 3404 cm^{-1} and 3399 cm^{-1} is assigned to NH_2 stretching vibration in pure and doped L-Cys.HCl.H_2O. The broad spectra which are observed at 2925 cm^{-1} and 2945 cm^{-1} is assigned to the O-H stretching in pure and doped L-Cys.HCl.H_2O. The S-H stretching appeared in pure at 2539 cm^{-1} is shifted to 2559cm^{-1} in Mn^{2+}: L-Cys.HCl.H_2O and also found C-H stretching at 2361 cm^{-1}. The sharp and strong peak observed at 1750 cm^{-1} indicates the C=O stretching of carbonyl group. The FTIR clearly shows an appreciable shift in C-S stretching from 613 to 643 cm^{-1} in Mn^{2+} doped crystal. Based on these shifts in stretchings, the presence of Mn^{2+} in the crystal lattice of L-Cys.HCl.H_2O is clearly evident. From these observations, it is concluded that S-H and C-S functional groups are directly involved in Mn coordination through S-ligand in L-Cys. HCl.H_2O [5].

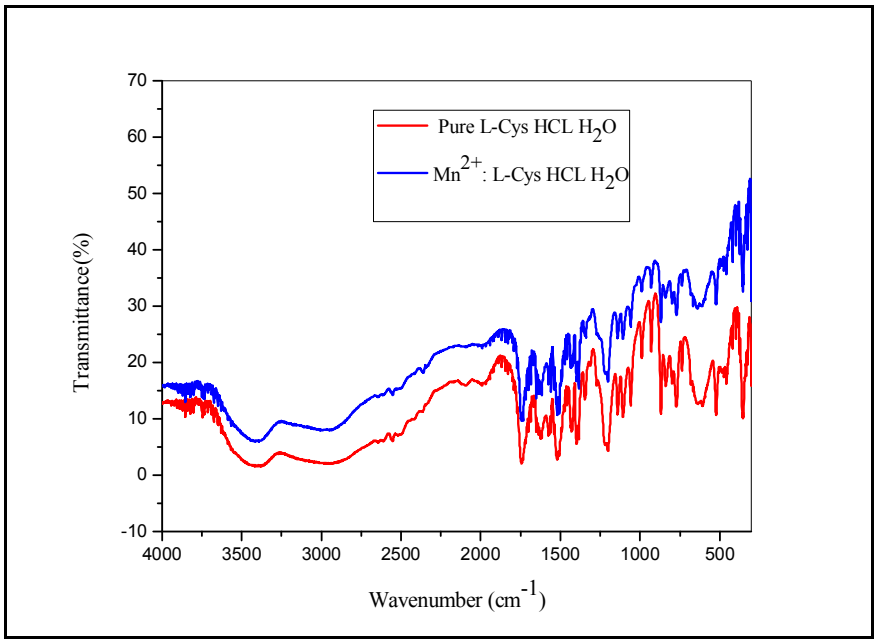

Fig. 3 FT-IR spectrum of the grown pure and Mn^{2+}: L-Cys.HCl.H_2O

UV-Vis Transmittance Studies:

The transmittance spectra of pure and Mn^{2+}: L-Cys.HCl.H_2O single crystals were shown in Fig. 4. For the pure L-Cys.HCl.H_2O the UV cutoff wavelength is found at 255 nm and Mn^{2+}: L-Cys.HCl.H_2O shows a slight shift in UV cutoff wavelength to 250 nm. From these results, it is evident that the dopants have an influence in the cut-off wave-length of the pure crystal.

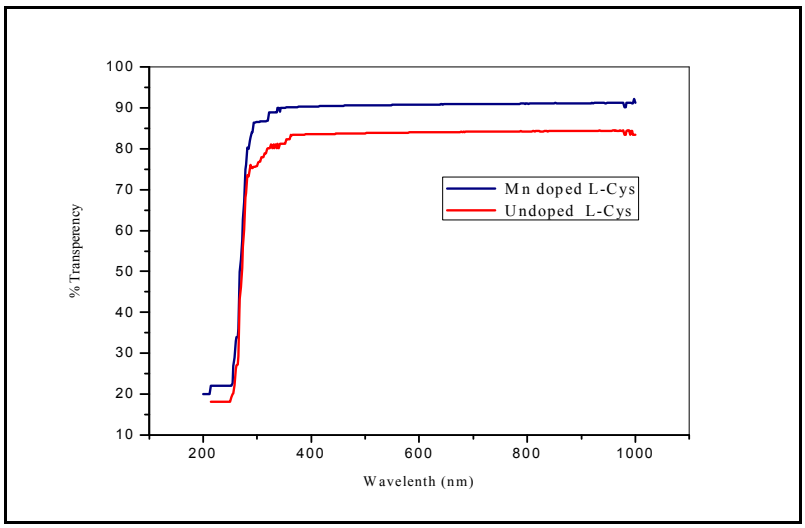

Fig. 4 : The UV-Vis transmission spectrum of Mn^{2+} doped and pure L-Cys HCl.H_2O crystal

Second Harmonic Studies (NLO):

The Second Harmonic Generation (SHG) test on the Mn^{2+}: L-Cys.HCl.H_2O crystal was performed by Kurtz powder technique [18]. The randomly oriented micro crystals of Mn^{2+}: L-Cys.HCl H_2O single crystal was irradiated using the fundamental beam of 1064 nm from Q-switched Nd: YAG laser. The energy of theincident laser beam is 2.5 mJ/pulse and pulse width about 10 ns with a repetition rate of 10 Hz. The second harmonic signal was about 15 mV. But the standard KDP crystals gave an SHG of 10 mV/pulse from the same input energy. Hence, it is seen that the SHG efficiency of Mn^{2+}: L-Cys.HCl H_2O crystal is 1.5 times that of the pure KDP crystal. The output could be seen as a bright green color emission from the sample. The green emission confirmed the second harmonic generation in the grown crystals and the metal doping influenced the efficiency of undoped L-Cys.HCl.H_2O.

Conclusion:

The powdered XRD, HRXRD, FTIR and Kurtz technique reveals the influence of Mn^{2+}: L-Cys.HCl.H_2O single crystals. The powder X-ray diffraction analysis of doped samples showed minor structural variations. FTIR studies showed the incorporation of Mn^{2+} ions through S-group in L-Cys.HCl.H_2O and also confirm the functional groups in pure and doped samples. High resolution XRD of the metal doped crystal had reasonably crystalline perfection and free from grain boundaries. HRXRD also confirms the incorporation of Mn^{2+} in the crystal lattice. The nonlinear optical character of the title compound was observed by measuring the SHG efficiency, which is 1.5 times of KDP as assessed by Kurtz technique. UV-vis spectrum showed that there is a slight change in the cut-off wavelength for doped crystal. From these observations, it can be concluded that the influence of metal ion enhances the optical transparency, SHG efficiency and hence doped crystals are promising materials for laser technology and may be used as electro-optic modulators.

Acknowledgements:

The authors are grateful to Dr. G. Bhagavannarayana, NPL Delhi for HRXRD studies. KRR is grateful to Dr. V. Sudarshan, Baba Atomic Research Centre, Mumbai for XRD and FTIR studies and Dr. Sunil Verma, RRCAT, Indore for his valuable suggestions. KRR also wishes to thank Prof. P. K. Das, IASc, Bangalore and Dr.Ch. Mastanaiah, Principal, Government College(A), Rajahmundry, Andhra Pradesh for SHG measurements and Lab facilities.

References

1. Dhumane N.R., Hussaini S.S., Dongre V.G., Ghugare P. and Shirsat M.D., Appl. Phys. 2009, A95, 727.
2. Kang H., Xi Yang C., Mu G. and Kang Z., Opt. Lett. 1990, 15, 637.
3. La Rocca G.C., Nat. Photonics 2010, 4, 343.
4. Chapman R.P. and Bryce D.L., Phys. Chem. Chem. Phys. 2007, 9, 6219.
5. Jason G.P., Kenneth M.D., McClure J. and Jorge L., Polyhedron 2013, 56.
6. Zuo F., Zhang B., Tang X. and Xie Y., Nanotechnology 2007, 18, 215608 (6pp).
7. Ashwell G.J., Jefferies G., Hamilton D.G., Lynch D.E., Roberts M.P.S., Bahra G.S. and Brown C.R., Nature 1995, 375, 385.
8. Ramirez M.O., Jaque D., Bausa L.E., Garcia Sole J. and Kaminskii A.A., Phys. Rev. Lett. 92005, 5, 267401.
9. Lim D., Downer M.C., Ekerdt J.G., Arzate N., Mendoza B.S., Gavrilenko V.I. and Wu R.Q., Phys. Rev. Lett. 2000, 84, 3406.
10. Soljacic M. and Joannopoulos J.D., Nat. Mater. 2004, 3, 211.
11. Loutts G.B., Warren M., Taylor L., Rakhimov R.R., Ries H.R., Miller G., Noginov M.A., Curley M., Noginova N., Kukhtarev N., Caulfield H.J. and Venkateswarlu P., Phys. Rev. B 1998, 57, 3706.
12. Krambrock K., Guedes K., Ladeira L.O., Benzerra M.J.B., Oliveira T.M., Benzerra G.A., Cavada B.S., de Oliveira M.C.F., Flores M.Z.S., Farias G.A. and Freire V.N., Phys. Rev. B 2007, 75, 104205.
13. Lal K. and Bhagavannarayana G., J. Appl. Cryst. 1989, 22, 209.
14. Bhagavannarayana G., Suman Kumar, MohdShakir, Kushawaha S.K., Maurya K.K., Rajni M. and Ramachandra Rao K., J. Appl. Cryst. 2010, 43, 710.
15. Batterman B.W. and Cole H., Rev. Mod. Phys, 1964, 36, 681.
16. Bhagavannarayana G., et al., J. Appl. Cryst. 2005, 38, 448.
17. Kushwaha S.K., et al., J. Crys. Growth 2011, 328, 81.
18. Kurtz S.K. and Perry T.T., J. Appl. Phys. 1968, 39, 3798.

*****